

## MANEUVERABLE TARGET TRACKING VIA OPTIMAL LQR CONTROLLER WITH TIME-VARYING RICCATI FEEDBACK AND TARGET STATE ESTIMATIONS

Onur Özgür<sup>1</sup>  
Aselsan Inc.  
Ankara, Turkey

### ABSTRACT

*In this study, a novel implementation of Linear Quadratic Regulator (LQR) controller is conducted in order to track a maneuverable target. The guidance command of the pursuer is determined by the feedback of real-time Riccati equation solutions during the pursuit. For this purpose, time-varying engagement kinematics accompanied by nonlinear terms are derived and introduced in state-space representation. Due to the fact that the control strategy requires range-to-target, target velocity and target acceleration estimations, a third-order digital fading memory filter is incorporated to predict the kinematic states of the target. Range and line-of-sight (LOS) information are assumed to be provided by a seeker mounted onboard the pursuer. As a consequence, it is shown that the pursuer can well be guided towards a maneuvering evader for a successful hit.*

### INTRODUCTION

Linear quadratic regulators can be defined as well-known optimal control based techniques to acquire decent feedback gains so that the states of the dynamic system are driven towards the desired values in an optimal manner.

Optimal control policy is determined by making use of a properly constituted cost function which may involve terms regarding the measured system states as well as the control input itself in a quadratic form. The terms may also be multiplied by weighting factors in order to adjust the state's regulation trends. The minimization process of this objective function results in optimal feedback gains that can be used to form the control variable which is likely to force the available system states to behave in intended manners.

Linear quadratic control is mainly used in path following and waypoint tracking during midcourse phase of the guidance. In [1], straight trajectories in between successive waypoints are tracked via implementation of a linear quadratic regulator wherein a set of linearized state equations are used with time-invarying system matrix. In [2], a hybrid lateral guidance law composed of LQR and PNG (*i.e. Proportional Navigation Guidance*) is designed to follow the desired trajectory towards waypoints.

---

<sup>1</sup> Senior Engineering Specialist at Microelectronics, Guidance and Electro-Optics Business Sector,  
Email: oozgur@aselsan.com.tr

In this work, LQR problem is reformulated with a novel insight to be applied on a maneuvering pursuer-evader pursuit engagement in which nonlinear and time-varying kinematic terms are used to obtain real-time Riccati solutions and estimated variables corresponding to the target's states take part in the derived system equations.

### STATE SPACE REPRESENTATION OF THE PURSUIT KINEMATICS

The states of the pursuit-evasion engagement are chosen so that the missile can guide itself towards the intended target and hit it eventually. A typical engagement scenario is depicted in Figure 1 to serve as a reference while deriving the differential state equations of the guidance problem. For simplicity, the engagement is considered to take place in a plane and the speeds of the pursuer and the evader are taken to be constant throughout the pursuit. Then, in order to form a maneuvering target concept, an acceleration that remains always perpendicular to the velocity of the evader is applied. Likewise, while modelling the kinematics of the pursuer, the control input, namely the acceleration vector, is taken to be perpendicular to missile's velocity vector. As indicated before, the range-to-target ( $R$ ) and line-of-sight angle ( $\lambda$ ) data are assumed to be known quantities via utilization of a seeker device.

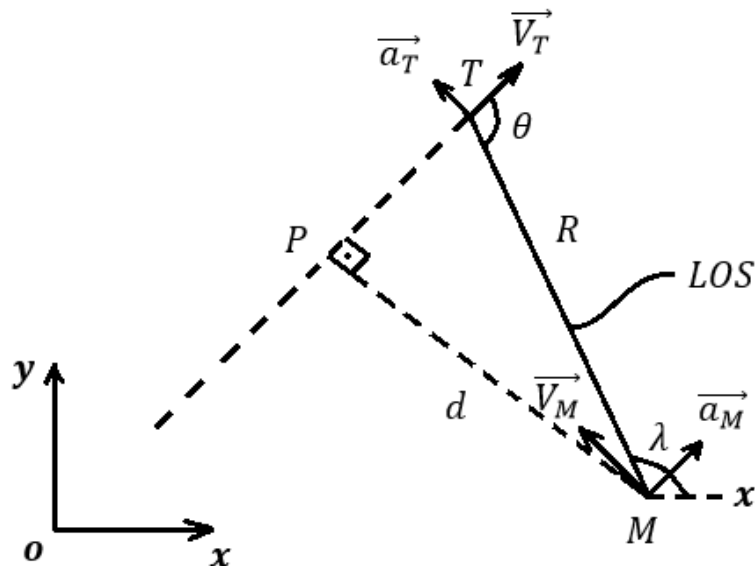


Figure 1: Pursuer-evader guidance engagement scenario

While selecting the states to be minimized for the problem in hand, two criteria are taken into account. One of them is the velocity vector alignment of the pursuer with respect to the evader and the second one is the pursuer's instantaneous distance to the line extension of the velocity vector of the evader. In other words, if the missile can direct its velocity vector to be parallel to the target's velocity vector responsively and in addition to that, if the missile can null the perpendicular distance ( $d$ ) to the target's velocity vector, then a successful hit is possible. It can be concluded that a tail-chase pursuit of the evader and a collision are likely to occur if these two criteria are met assuming that both the speed and maneuverability of the missile are superior to the target.

From above discussion, one of the states may be selected as a function of the angle difference in between pursuer's and evader's velocity vectors. The ground track angles of the missile and the target together with the difference in between them as denoted by  $\varphi$  can be seen in Figure 2. The second state can be selected as the distance labeled as  $d$  in Figure 1. Lastly, the control input ( $\bar{a}_M$ ) can be taken as the third state to play role in the state-space representation of the pursuit kinematics so that the calculated acceleration values can be directly applied on the

velocity vector of the missile to guide it towards the maneuvering target while regulating the other two state variables towards zero.

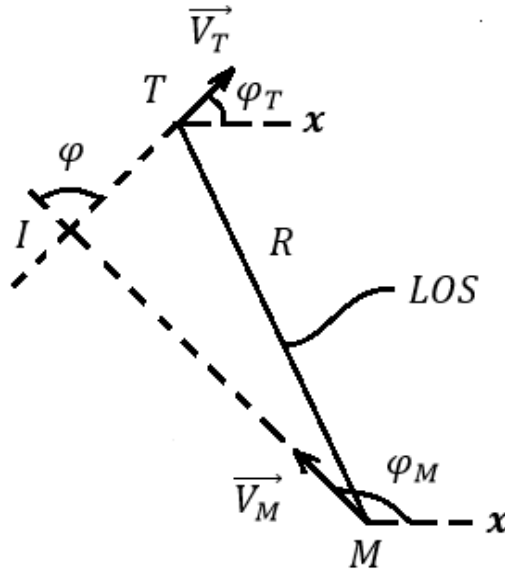


Figure 2: Ground track angle definitions corresponding to target and missile

Choosing the first state as a multiplication of missile's speed and the angle difference  $\varphi$ , state variables  $(s, d, a)$  can be expressed as the following.

$$s = V_M(\varphi_M - \varphi_T)$$

$$\varphi = \varphi_M - \varphi_T$$

$$s = V_M \varphi$$

$$d = R \sin(\theta)$$

$$a = a_M$$

State equations as a set of first-order differential equations can be derived as given below where  $\mathbf{u}$  stands for the control input provided by the algebraic Riccati equation (ARE) solutions and  $\tau$  can be interpreted as autopilot's time constant.

$$\dot{s} = V_M(\dot{\varphi}_M - \dot{\varphi}_T)$$

$$\dot{d} = \dot{R} \sin(\theta) + R \cos(\theta) \dot{\theta}$$

$$\dot{a} = -a_M/\tau + u/\tau$$

As mentioned before, the acceleration vectors are applied perpendicular to the velocity vectors of the pursuer and the evader yielding the equalities below.

$$\dot{\varphi}_M = a_M/V_M$$

$$\dot{\varphi}_T = a_T / V_T$$

Substitution of these equalities into the first state equation, the following expression holds true.

$$\dot{s} = V_M \left( a_M / V_M - \hat{a}_T / \hat{V}_T \right)$$

Further simplifications can be made to obtain the final form of the state equation. In these expressions, the overscript (^) is used to identify the estimated terms.

$$\dot{s} = a_M - \hat{a}_T (V_M / \hat{V}_T)$$

For the second state equation, an equivalent derivation can be made since the Hamiltonian spectrum becomes too close to the imaginary axis due to the derivative terms, thus making the Riccati equation unsolvable. Alternative derivation allows to express the state ( $d$ ) in terms of one of the first state variables ( $\varphi$ ).

$$\dot{d} \cong -V_M \sin \varphi - (\dot{\varphi}_T)(R \cos(180 - \theta))$$

$$\dot{d} \cong -V_M \sin \varphi + \left( \hat{a}_T / \hat{V}_T \right) R \cos(\theta)$$

By making use of small angle approximation for the angle difference ( $\sin(\varphi) \approx \varphi$ ) and utilizing the fact that  $\cos(\theta) \approx -1$  during tail-chase pursuit, the second state equation can be simplified to the following.

$$\dot{d} \cong -V_M \varphi + R \left( \hat{a}_T / \hat{V}_T \right)$$

However, in the presented implementation as claimed before, nonlinear terms will be held while forming state-space representation of the dynamical system. The general form of the representation for the dynamical system is given below.

$$\dot{x}(t) = A(t)x(t) + B(t)u(t)$$

Time-varying system and control input matrices can be represented as below in compact form.

$$A(t) = \begin{bmatrix} 0 & 0 & \left[ 1 - (\hat{a}_T / a_M) (V_M / \hat{V}_T) \right] \\ \left[ -V_M \sin(\varphi) + \left( \hat{a}_T / \hat{V}_T \right) R \cos(\theta) \right] / (V_M \varphi) & 0 & 0 \\ 0 & 0 & -1/\tau \end{bmatrix}$$

$$B(t) = \begin{bmatrix} 0 \\ 0 \\ 1/\tau \end{bmatrix}$$

### QUADRATIC COST FUNCTION AND STATE-FEEDBACK VIA RICCATI SOLUTIONS

Estimated states together with measured control variable constitute the cost function  $J$  in quadratic form to the minimization problem.

$$J = \int_0^{t_f} (x'Qx + u^2) dt$$

$$x = \begin{bmatrix} s \\ d \\ a \end{bmatrix}$$

$$Q = \begin{bmatrix} q_1 & 0 & 0 \\ 0 & q_2 & 0 \\ 0 & 0 & 0 \end{bmatrix}$$

The diagonal elements  $q_1$  and  $q_2$  of the  $Q$  matrix that can be described as the weighting factors enable the control designer to tune the characteristics of the trajectory to be followed by the pursuer. Selection of  $q_1$  as the dominant factor is likely to force the pursuit kinematics in a way that the angle difference in between the velocity vectors of the pursuer and the evader is to be zeroed as the primary objective whereas  $q_2$  factor is related to the reduction rate in the distance  $d$ . It is possible to generate distinct pursuer trajectories with the selection of different weighting factor combinations. In the scope of this work, the weighting factors are optimized to satisfy minimum miss distance requirement.

The control variable  $u$  is generated via state-feedback of optimal gain  $K$ . In order to apply guidance commands successfully, state variables need to be measured or estimated continuously and supplied to the guidance controller simultaneously.

$$u = -Kx$$

$$K = (B^T P)$$

$$u = -(B^T P)x$$

The positive definite matrix  $P$ , whose eigenvalues are all positive real numbers, is calculated from the solution of the below algebraic Riccati equation. A constant  $P$  matrix is obtained provided that both system matrix  $A$  and weighting matrix  $Q$  are taken to be time-invariant. Time-varying Riccati equation solutions can be determined online while flying towards the target, as the case presented in this work, if system matrix  $A$  involves terms changing with time.

$$A^T P + PA - (PB)(PB)^T + Q = 0$$

### TARGET STATE ESTIMATOR

Target states including the components of position, velocity and acceleration can be estimated for distinctive motion types of maneuvering target via range-to-target and line-of-sight measurements provided by an onboard seeker [3].

In this study, a third-order digital fading memory is implemented for this purpose. Recursive filter equations [4] together with a generic block diagram are presented below for convenience.

$$\hat{x}_n = \hat{x}_{n-1} + \hat{\dot{x}}_{n-1}T_s + 0.5\hat{\ddot{x}}_{n-1}T_s^2 + G_F[x_n^* - (\hat{x}_{n-1} + \hat{\dot{x}}_{n-1}T_s + 0.5\hat{\ddot{x}}_{n-1}T_s^2)]$$

$$\hat{\dot{x}}_n = \hat{\dot{x}}_{n-1} + \hat{\ddot{x}}_{n-1}T_s + \frac{H_F}{T_s}[x_n^* - (\hat{x}_{n-1} + \hat{\dot{x}}_{n-1}T_s + 0.5\hat{\ddot{x}}_{n-1}T_s^2)]$$

$$\hat{\ddot{x}}_n = \hat{\ddot{x}}_{n-1} + \frac{2K_F}{T_s^2}[x_n^* - (\hat{x}_{n-1} + \hat{\dot{x}}_{n-1}T_s + 0.5\hat{\ddot{x}}_{n-1}T_s^2)]$$

$$G_F = 1 - \beta^3$$

$$H_F = 1.5(1 - \beta)^2(1 + \beta)$$

$$K_F = 0.5(1 - \beta)^3$$

In these equations,  $\hat{x}$  stands for the estimated states whereas  $x^*$  represents the noisy seeker measurements.  $T_s$  and  $\beta$  parameters are fine-tuned to ensure that the filter acts quickly and eliminates the excessive noise related to the measurements, respectively.

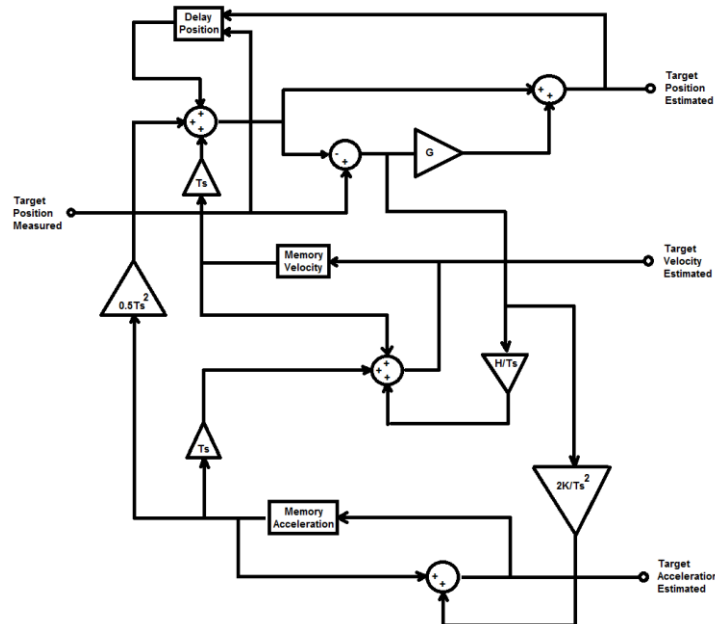


Figure 3: Third Order Fading Memory Filter Block Diagram

In order to evaluate the performance of the filter in eliminating the excessive noise in the measurements and predicting the states of the maneuvering target, line-of-sight and range measurements are corrupted by random Gaussian noise of  $10^\circ$  and 100 meters variances,

respectively. Due to the fact that seeker measurements generally gets more precise as range-to-target decreases, noise levels are reduced intentionally as the pursuer gets closer to the target. Filter parameters are tuned to match the estimated states with the real ones as early and accurate as possible.

The implemented filter requires initial guesses corresponding to the velocity and acceleration components of the target. Assuming that this knowledge is not available to the pursuer at the beginning of the engagement,  $[20, 15]$  [m/s] and  $[0.3, 0.5]$  [m/s<sup>2</sup>] values are assigned as the initialization conditions regarding the velocity and acceleration components of the target, respectively.

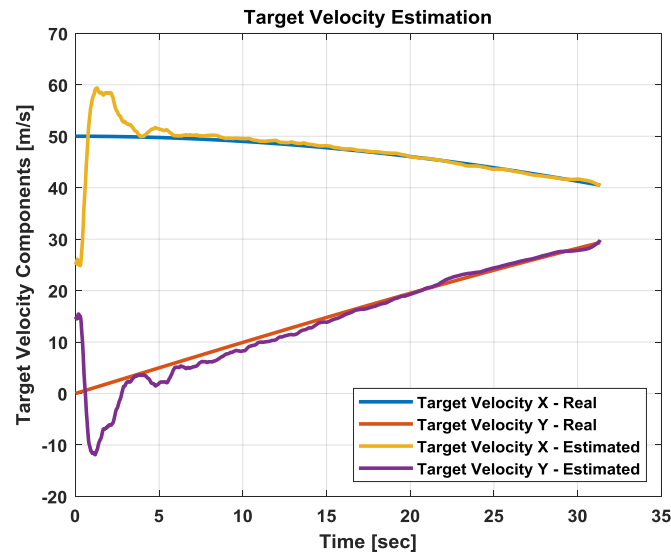


Figure 4: Target Velocity Estimation

Due to huge velocity differential in between the real state values and the initial guesses, steep jumps are likely to be observed for the first few seconds of the engagement. These jumps can be prevented provided that initial guesses gets more accurate. Nevertheless, target states were able to be estimated with satisfactory results within 3-4 seconds. A wise strategy to deal with this predicament could be letting the filter estimations take role in the closed guidance loop after a while, once the estimated state rates drop to lay within acceptable bounds.

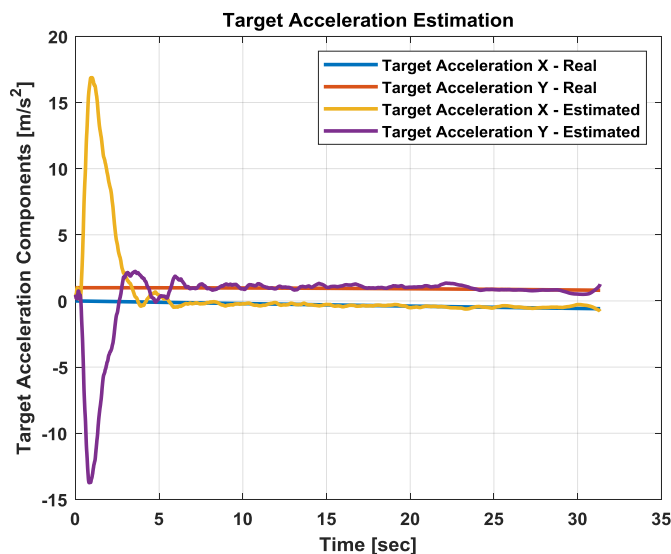


Figure 5: Target Acceleration Estimation

## SIMULATION RESULTS

In this section, the trajectories of the pursuer and the evader belonging to different guidance scenarios with distinct initialization parameters are plotted to illustrate the achievement of the proposed algorithm in guiding the missile towards a maneuvering target.

Figure 6 shows the variation of the trajectories which eventually ends up with a successful hit. For this scenario, the missile is directed towards the target at the launch and then, its trajectory deviates from the initial line-of-sight while tracking a maneuvering target. The speeds of the missile and the target are taken to be 70 m/s and 50 m/s, respectively. The target is assumed to maneuver with 1 m/s<sup>2</sup> acceleration perpendicular to its velocity vector resulting in approximately 1.15 deg/s change in ground track. The simulation lasted 32 seconds with a miss distance of 0.36 meters.

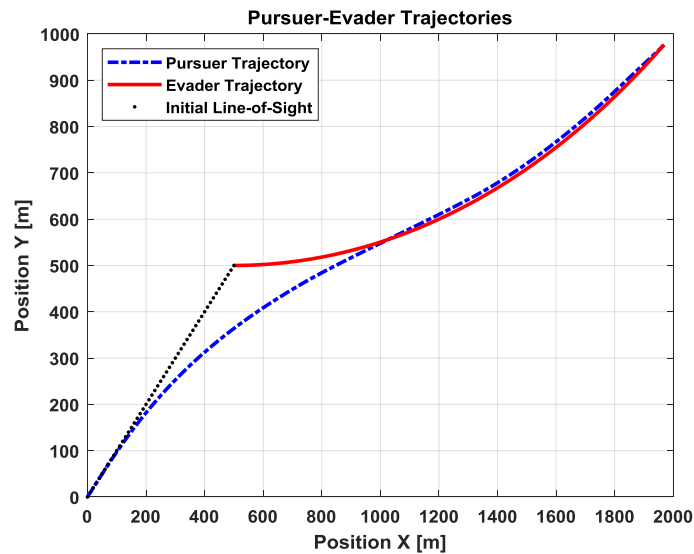


Figure 6: Pursuer-Evader Trajectory – First Case

It can be concluded from Figure 7 that an acceleration advantage of about 3 times is required by the missile to track and hit the target effectively.

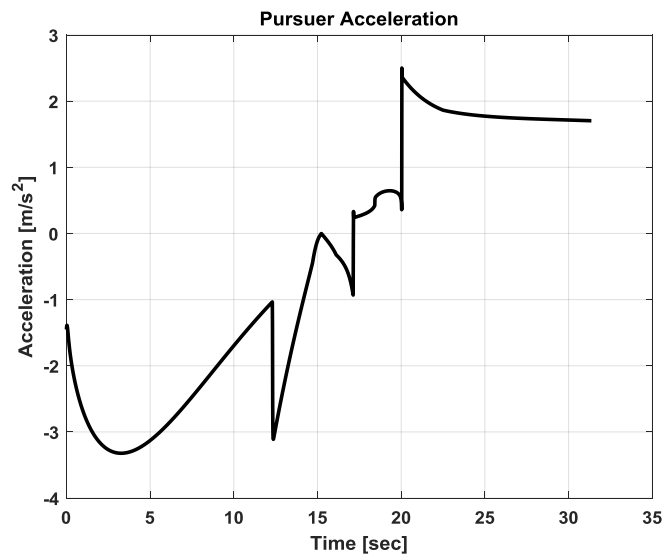


Figure 7: Pursuer Acceleration – First Case



Figure 8 shows the variation of the angle in between the velocity vectors of the pursuer and the evader throughout the engagement. It is seen that the  $45^\circ$  of difference is almost zeroed with a final value of  $1.5^\circ$  at the end of the pursuit.

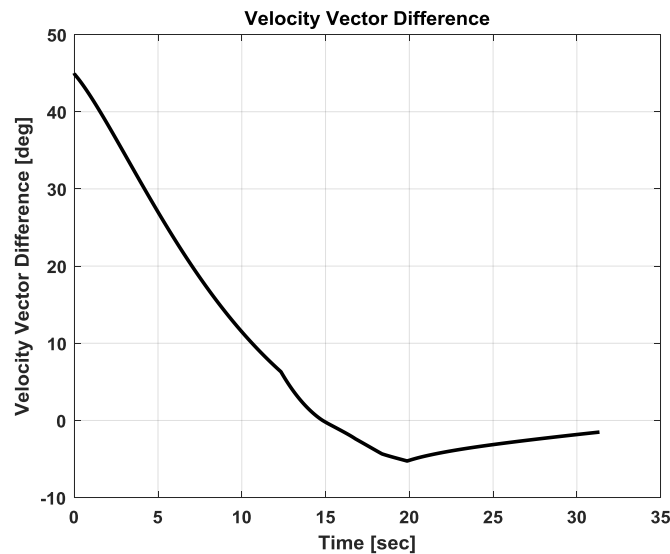


Figure 8: Velocity Vector Difference – First Case

The distance to ensure a tail-chase following of the target starts with a value of 500 meters and it is driven towards the miss distance as can be seen in Figure 9.

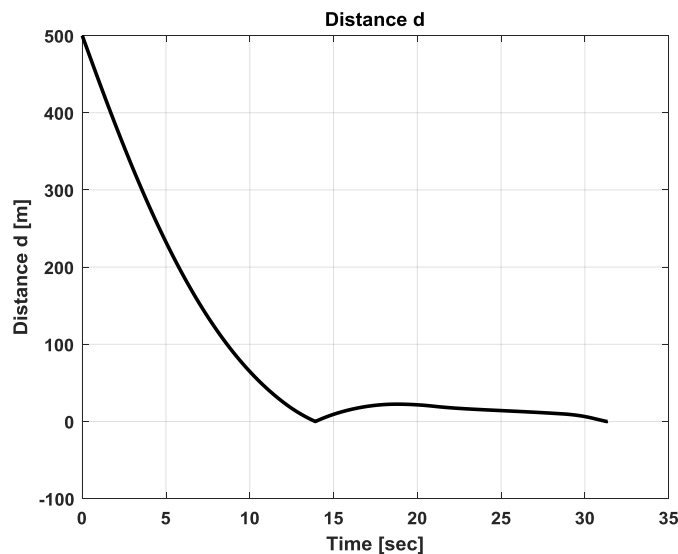


Figure 9: Distance  $d$  – First Case

To sum up, the angle and distance states of the LQR problem are seen to converge to zero as a result of the acceleration being applied perpendicular on the pursuer velocity vector. As a consequence, the missile is seen to track the maneuvering target leading to a tail-chase pursuit and ending up with an accurate hit while making use of missile's speed advantage over the target.

The following figures demonstrate trajectories generated in relation to different engagement scenarios.

Figure 10 shows the effect of weighting factors on the path being followed by the pursuer. In this scenario, distance minimization is weighted to be more effective compared to the first case

and a different trajectory is obtained which aims to null the distance  $d$  at early stages of the engagement also resulting in better angular tracking at the terminal phase of the engagement.

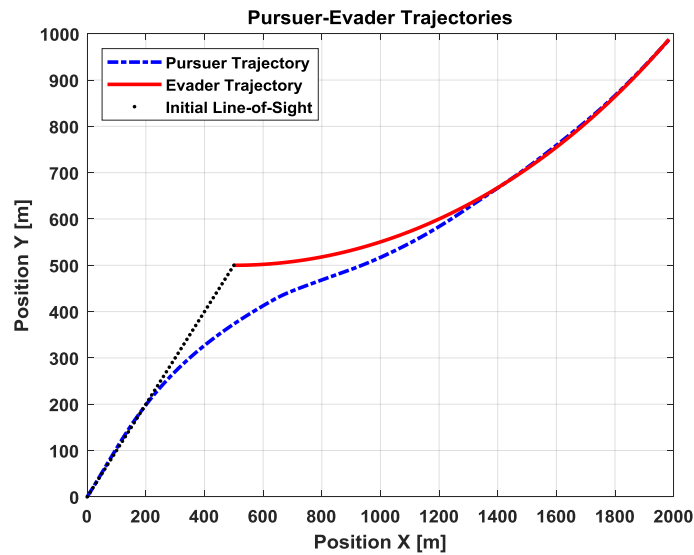


Figure 10: Pursuer-Evader Trajectories – Second Case

Figure 11 demonstrates the effect of missile’s launch angle on the trajectory being followed. In this scenario, missile is launched in the upward direction with a  $45^\circ$  of heading error compared to the initial line-of-sight. Afterwards, missile maneuvers to guide itself to remain in a tail-chase collision course.

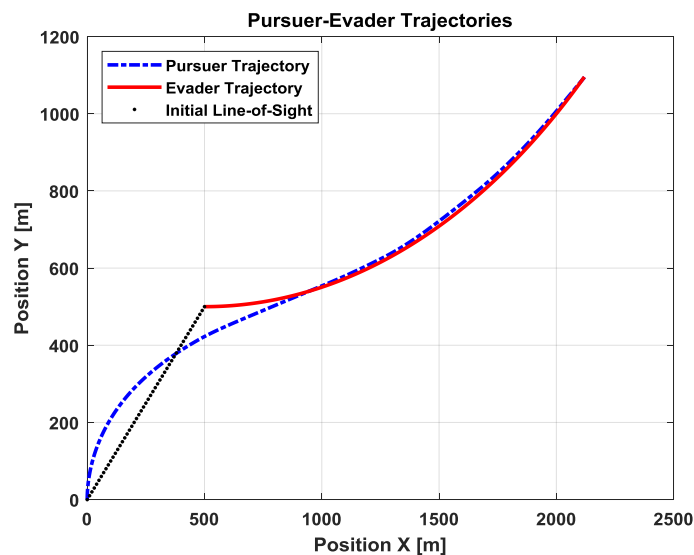


Figure 11: Pursuer-Evader Trajectories – Third Case

In Figure 12, another launch angle is assigned for the missile yielding a more direct guidance towards the target. In all these engagement scenarios, miss distance value of below 3 meters which is considered to be successful is obtained.

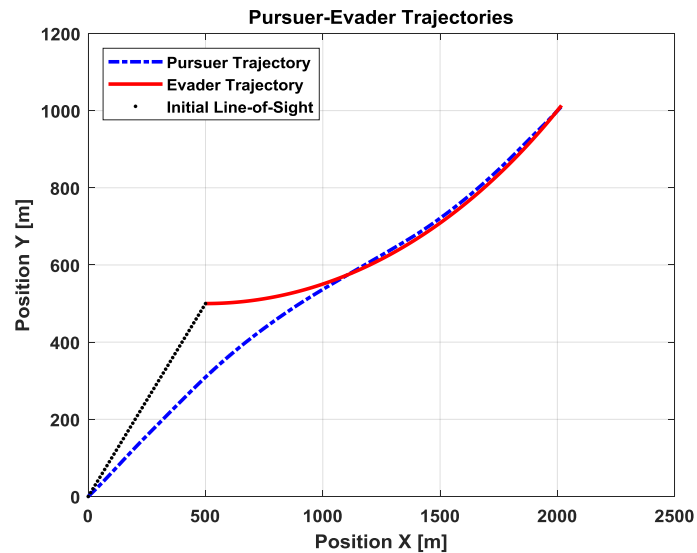


Figure 12: Pursuer-Evader Trajectories – Fourth Case

In Figure 13, the missile is launched with a greater heading error compared to the fourth case.

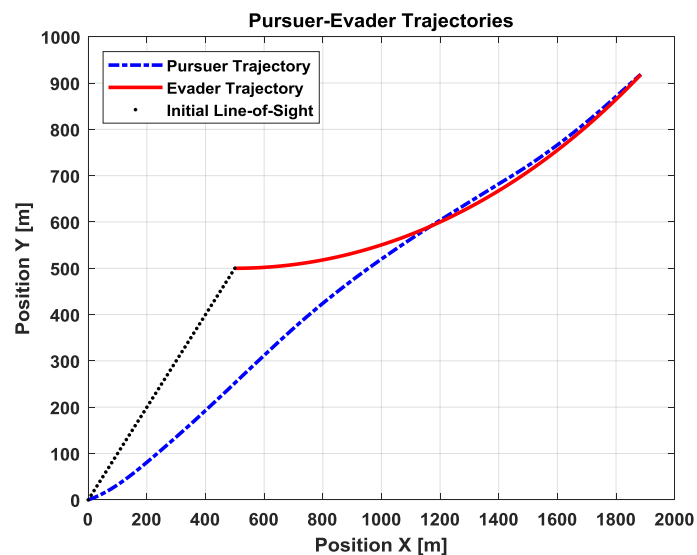


Figure 13: Pursuer-Evader Trajectories – Fifth Case

Figure 14 exemplifies that the developed algorithm may also be implemented for cases where the evader does not maneuver but travels along a fixed direction.

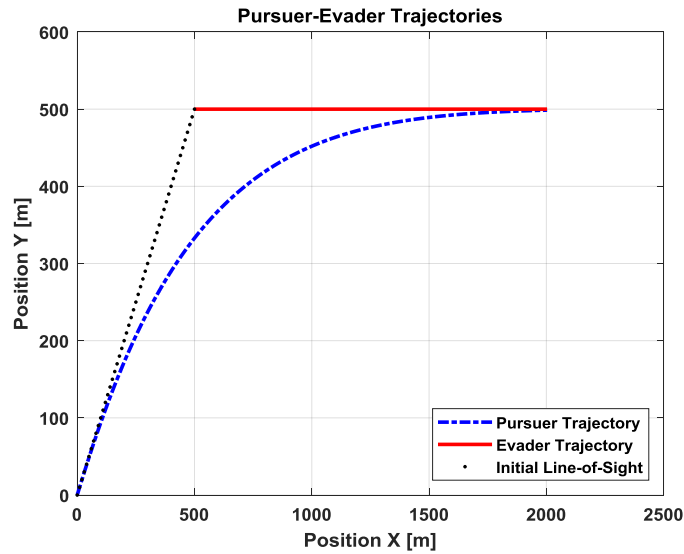


Figure 14: Pursuer-Evader Trajectories – Sixth Case

For the case illustrated in Figure 15, the speeds of the pursuer and the evader are doubled in comparison to the first case, which results in smaller ground track angular variation in target's motion.

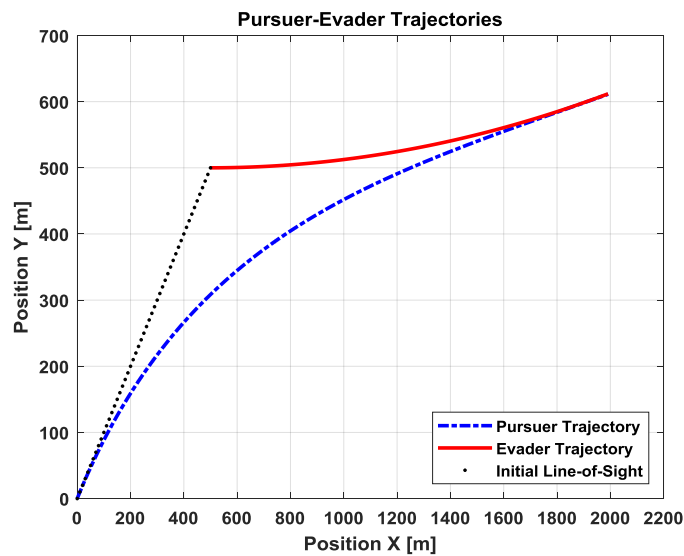


Figure 15: Pursuer-Evader Trajectories – Seventh Case

Figure 16 demonstrates a case wherein the initial range in between the pursuer and the evader is doubled in comparison to the first case, which gives the pursuer more time to correct its course.

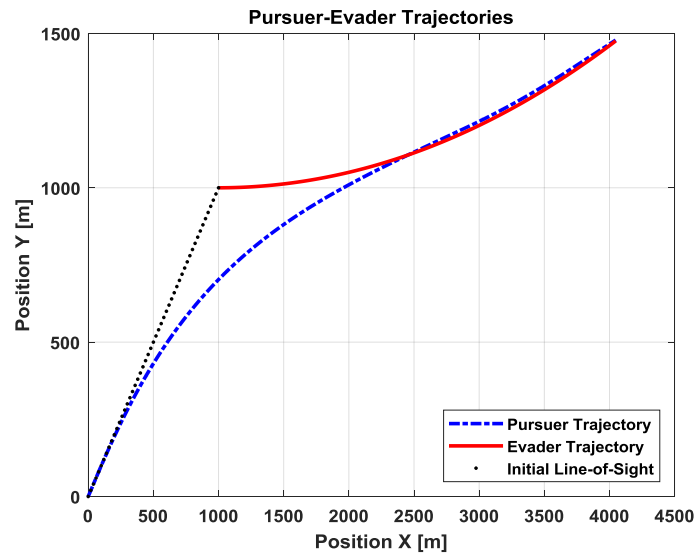


Figure 16: Pursuer-Evader Trajectories – Eighth Case

In the ninth case, the acceleration magnitude of the evader is doubled to  $2 \text{ m/s}^2$  yielding of about  $2.3 \text{ deg/s}$  change in ground track while enhancing the maneuverability of the target.

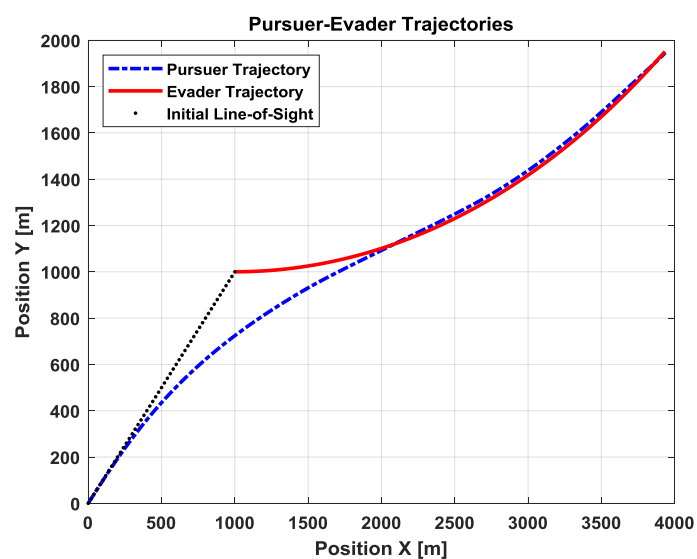


Figure 17: Pursuer-Evader Trajectories – Ninth Case

Figure 18 depicts a guidance scenario in which the target starts its motion with a constant speed along a straight line and then, when the missile gets in the close vicinity of the target, the target maneuvers to get rid of the chasing missile.

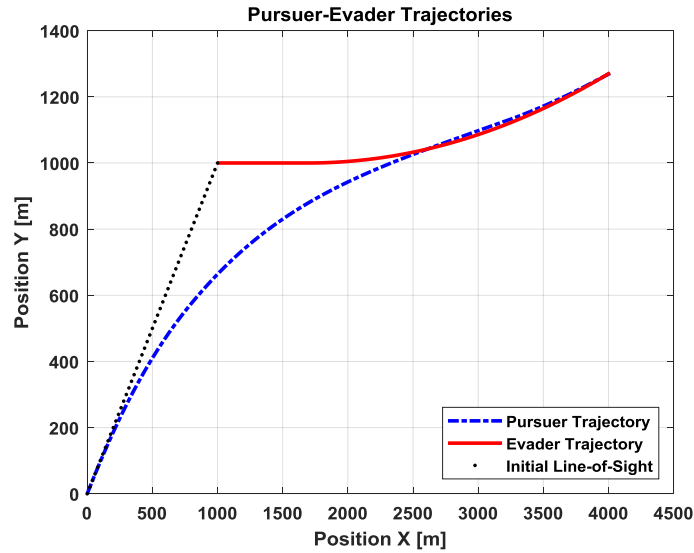


Figure 18: Pursuer-Evader Trajectories – Tenth Case

In Figure 19, the initial range-to-target is much greater than the ones in the cases scrutinized so far. This situation allows to see clearly the deviation in the missile’s trajectory to null the distance and angle states during the mid-phase of the pursuit for a successful interception.

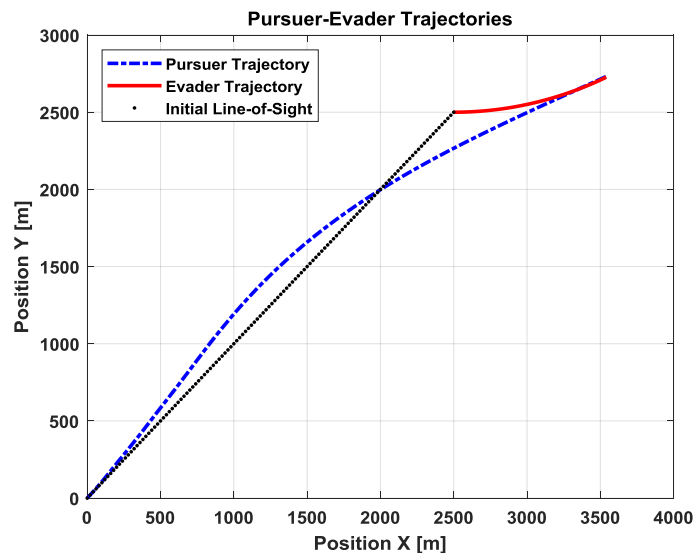


Figure 19: Pursuer-Evader Trajectories – Eleventh Case

## DISCUSSION AND CONCLUSION

In this study, kinematic relations in between a pursuer and a maneuvering evader are derived in accordance with the LQR formulation. Nonlinear terms arising from the derivations are kept to take place in the state space representation of the system. Time-varying system matrix is used in formation of P matrices throughout the pursuit wherein Riccati feedback is calculated at each time step of the engagement. Weighting factors of the optimization problem are fine-tuned to ensure minimum miss distance values.

As the control method requires the estimated states of the target to be determined from noisy sensor measurements, a well-known target estimator is implemented to serve as an example in prediction of the target states, including its velocity and acceleration components. Parameters of the filter are adjusted so that satisfactory estimation results are acquired.

The simulation results illustrating the trajectories of the evader and the pursuer are presented for distinct initialization parameters. The effects of initial conditions on the generated trajectories are discussed. The variation of system states are depicted as they are driven towards zero to show the effectiveness of the proposed formulation in tracking a maneuvering target.

Consequently, it is demonstrated that a maneuvering target can be tracked successfully resulting in a tail-chase engagement and the target can be hit with quite good precision while taking speed and maneuverability advantage of the pursuer over the target into consideration.

## References

- [1] Hwang, T. W., Whang, I. H., *Horizontal Waypoint Guidance Design Using Optimal Control*, IEEE Transactions on Aerospace and Electronic Systems, Vol. 38, No. 3, Jul 2002.
- [2] Kim, T-H., Lee C-H., Tahk, M-J., *Real Time Path Planning Algorithm and Guidance Law for the Glider Bomb*, ICROS-SICE International Joint Conference, Japan, Aug 2009.
- [3] Ozgur, O. *The Effects of Random Seeker Noise and Target Maneuver on Guidance Performance*, Middle East Technical University, MSc. Thesis, Sep 2014.
- [4] Zarchan, P. *Tactical and Strategic Missile Guidance - Sixth Edition*, American Institute of Aeronautics and Astronautics, Vol. 239, Feb 2012.